

## Molecular Structures and Dynamic Behaviour of Two Isomers of $[\text{Ru}_3(\mu\text{-H})(\mu_3\text{-Me}_2\text{NC}_4\text{H}_4)(\text{CO})_9]$ formed from 1-Dimethylaminobut-2-yne and containing $\eta^2$ -Alkene-1,3-diyl and $\eta^2$ -Alkene-1,2-diyl Ligands Respectively †

Silvio Aime\* and Domenico Osella

*Istituto di Chimica Generale ed Inorganica, Università di Torino, Corso Massimo d'Azeglio 48, Torino 10125, Italy*

Antony J. Deeming\* and Alejandro J. Arce

*Department of Chemistry, University College London, 20 Gordon Street, London WC1H 0AJ*

Michael B. Hursthouse\* and Helen M. Dawes

*Department of Chemistry, Queen Mary College, Mile End Road, London E1 4NS*

Single-crystal *X*-ray structures of the isomeric compounds  $[\text{Ru}_3(\mu\text{-H})(\mu_3\text{-MeC=CCH=NMe}_2)(\text{CO})_9]$  (1) and  $[\text{Ru}_3(\mu\text{-H})(\mu_3\text{-MeC=CHC=NMe}_2)(\text{CO})_9]$  (2), both prepared from  $[\text{Ru}_3(\text{CO})_{12}]$  and the aminoalkyne  $\text{MeC}\equiv\text{CCH}_2\text{NMe}_2$ , have been determined. Isomer (1) formally contains the  $\mu_3$ - $\eta^2$ -alkyne  $\text{MeC}\equiv\text{CCH}=\text{N}^+\text{Me}_2$  which requires the associated negative charge of the zwitterion to be located at the ruthenium atoms.  $^{13}\text{C}$  n.m.r. spectra reveal localised dynamic exchange of axial and equatorial CO ligands at Ru atoms and these processes together with a rotation of the  $\mu_3$ -alkyne lead to a single  $^{13}\text{C}$  n.m.r. signal at +90 °C. The isomer (2) formed by heating (1), contains two 1,3-related Ru–C  $\sigma$  bonds and a  $\eta^2$ -alkene group. Although there is localised axial–equatorial CO exchange at two of the three Ru atoms, no  $\mu_3$  ligand rotation is observed in this case.

Alkynes of the type  $\text{MeC}\equiv\text{CCH}_2\text{R}$  (R = H or alkyl) react with  $[\text{Ru}_3(\text{CO})_{12}]$  by oxidative addition, with cleavage of a C–H bond adjacent to the triple bond, to give the  $\mu_3$ -allenyl cluster  $[\text{Ru}_3\text{H}(\text{MeC}=\text{C}=\text{CHR})(\text{CO})_9]$  which isomerises thermally by a 1,2-hydrogen atom shift to  $[\text{Ru}_3\text{H}(\text{MeCCHCR})(\text{CO})_9]$  as shown in Scheme 1. Similar behaviour is found for osmium.<sup>1,2</sup> The structures of the products have been fully established spectroscopically and by single-crystal *X*-ray structure determination in certain cases.<sup>3,4</sup> The related alkyne  $\text{MeC}\equiv\text{CCH}_2\text{R}$  with R =  $\text{NMe}_2$  also gives  $[\text{Ru}_3\text{H}(\text{MeCCCHNMe}_2)(\text{CO})_9]$ , compound (1), initially and this isomerises (rather more readily and at lower temperatures) to  $[\text{Ru}_3\text{H}(\text{MeCCHCNMe}_2)(\text{CO})_9]$  (2). The synthesis and basic characterisation of these isomers have already been described.<sup>5</sup> Superficially the chemistry with R =  $\text{NMe}_2$  is the same as with R = H or alkyl (Scheme 1), but we now report the *X*-ray structures and dynamic behaviour of isomers (1) and (2) which show notable differences from those of the related compounds with purely hydrocarbon ligands.

### Results and Discussion

**Structure and Dynamic Behaviour of Compound (1).**—A single-crystal *X*-ray structure determination clearly establishes the structure shown for compound (1) rather than the alternative  $\mu_3$ -allenyl structure (3) analogous to that found when there was an alkyl rather than an  $\text{NMe}_2$  substituent. The structure is shown in Figure 1 and selected bond lengths and angles are presented in Table 1. We regard the cluster as formally containing the  $\mu_3$ -alkyne  $\text{MeC}\equiv\text{CCH}=\text{N}^+\text{Me}_2$  bonded with two Ru–C  $\sigma$  bonds at Ru(1) and Ru(3) and a  $\eta^2$  interaction at Ru(2). The  $\text{Me}_2\text{N}=\text{CH}$  group contains a planar nitrogen atom (sum of angles 359.8°) and a short N–C(2) bond of 1.298(5) Å which rules out structure (3). The carbon atom C(2) is clearly not

directly bonded to ruthenium. The hydride ligand is located between Ru(1) and Ru(3), symmetrically within experimental error, the expected position for either the structure found for (1) or the alternative structure (3). The Ru(1)–Ru(3) distance of 2.978(1) Å is much greater than the other intermetal distances [2.723(1) and 2.742(1) Å]. Although the  $\mu_3$ -alkyne is close to being symmetrically bound [with an approximate mirror plane through Ru(2) if one ignores the different alkyne substituents], there is a small but distinct twist so that C(5) is associated with the shorter  $\sigma$  Ru–C bond and the longer Ru–C bond in the  $\eta^2$  interaction. The reverse is true for C(1). Such small twists are quite common and do not always arise from their being different substituents at the alkyne. The ligand is a four-electron donor with a negative charge formally at the metal atoms. Similar zwitterionic  $\mu_3$ -alkyne clusters have been observed before:  $[\text{Os}_3\text{H}(\mu_3\text{-MeC}=\text{CCH}_2\text{P}^+\text{Me}_2\text{Ph})(\text{CO})_9]$  and  $[\text{Os}_3\text{H}(\text{CO})_9(\mu_3\text{-HC}=\text{CP}^+\text{Me}_2\text{Ph})]$ .<sup>6</sup> The dimethylamino group is a good  $\pi$  donor and in two other clusters this donation has been shown to be sufficient to modify totally the ligand–metal bonding. The substituted vinyl cluster  $[\text{Os}_3\text{H}(\mu\text{-CH}=\text{CHR})(\text{CO})_{10}]$  where R =  $\text{NEt}_2$  does not adopt the same structure as when R = alkyl but rather the zwitterionic form with an alkylidene bridge,  $[\text{Os}_3\text{H}(\mu\text{-}\sigma\text{-CHCH}=\text{N}^+\text{Et}_2)(\text{CO})_{10}]$ .<sup>7,8</sup> Likewise the cluster  $[\text{Ru}_3\text{H}(\mu_3\text{-Me}_2\text{NC}=\text{C}=\text{CH}_2)(\text{CO})_9]$  does not adopt the normal  $\mu_3$ -allenyl structure (4) when R =  $\text{NMe}_2$  but rather the zwitterionic form  $[\text{Ru}_3\text{H}(\mu_3\text{-Me}_2\text{N}^+=\text{C}=\text{C}=\text{CH}_2)(\text{CO})_9]$ , structure (5).<sup>9</sup>

Cluster (1) is dynamic. At –85 °C the  $^{13}\text{C}$  (carbonyl) n.m.r. spectrum is consistent with the crystal structure and our assignments are given in Table 2; the signals for a and e coincide. The fastest intramolecular process, that observed between –85 and –50 °C, is the coalescence of signals for d, e, and f (coalescence of signals at 195.5, 193.8, and 207.8 p.p.m. to give one at 199.0 p.p.m.). Axial–equatorial CO exchange is localised at Ru(2) and faster than at the other metal atoms. Ru–CO bond lengths for the axial ligands at Ru(1) and Ru(3) are 1.932(6) and 1.946(6) Å respectively and longer than others in the molecule which vary between 1.879(6) and 1.922(6) Å. The *trans* influence of the  $\sigma$  Ru–C bonds between the  $\mu_3$  ligand and the metal atoms on the M–CO distances is greater than that of the  $\eta^2$  interaction

† Supplementary data available (No. SUP 56538, 6 pp.): thermal parameters, H-atom co-ordinates, H-atom bond lengths and angles. See Instructions for Authors, *J. Chem. Soc., Dalton Trans.*, 1986, Issue 1, pp. xvii–xx. Structure factors are available from the editorial office.

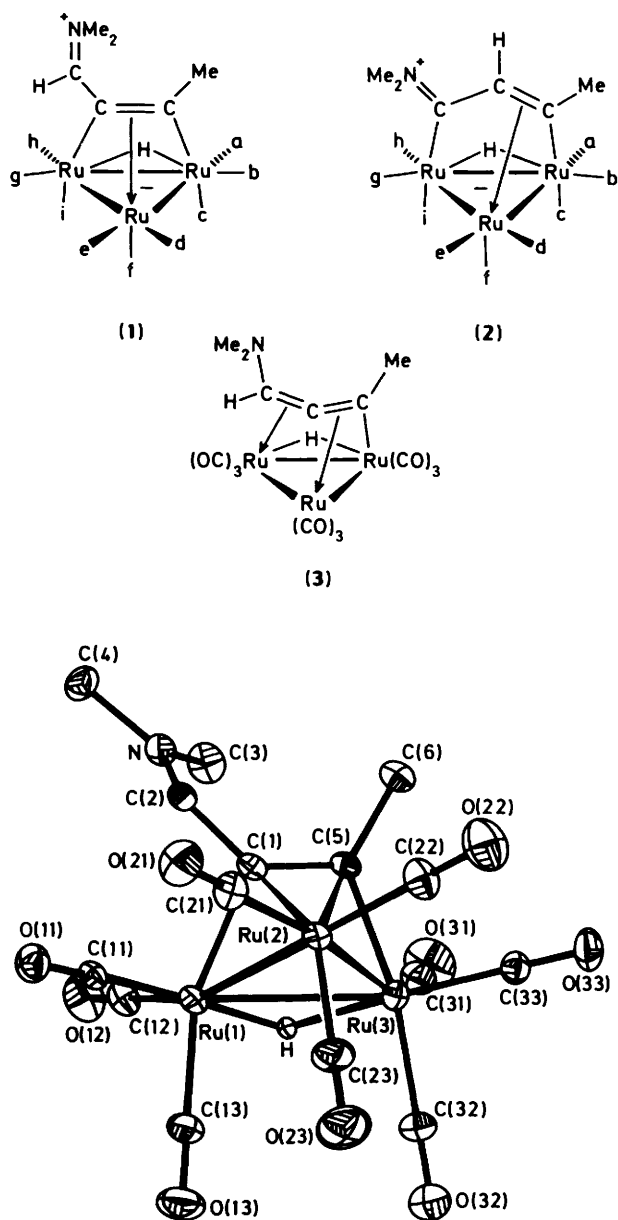
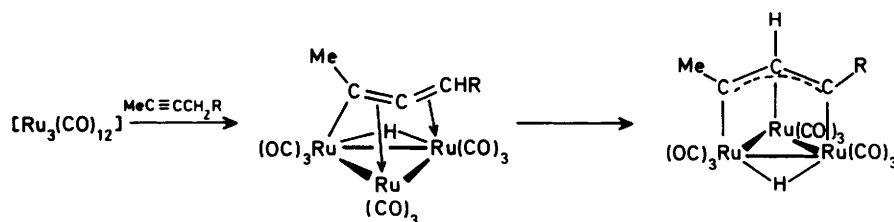


Figure 1. Structure of  $[\text{Ru}_3\text{H}(\text{MeC}=\text{CCH}=\text{NMe}_2)(\text{CO})_9]$  (1)

and this may relate to the faster axial-equatorial exchange at Ru(2). Between  $-50$  and  $+21$  °C another process occurs which exchanges carbonyls within the set d-i and also a with b. The oscillation of the  $\mu_3$  ligand as shown in Scheme 2 accounts for this observation. This oscillation interconverts enantiomers to generate a time-averaged plane of symmetry and this requires that the hydride ligand migrates in conjunction with the ligand

Table 1. Selected bond lengths (Å) and angles (°) for compound (1)

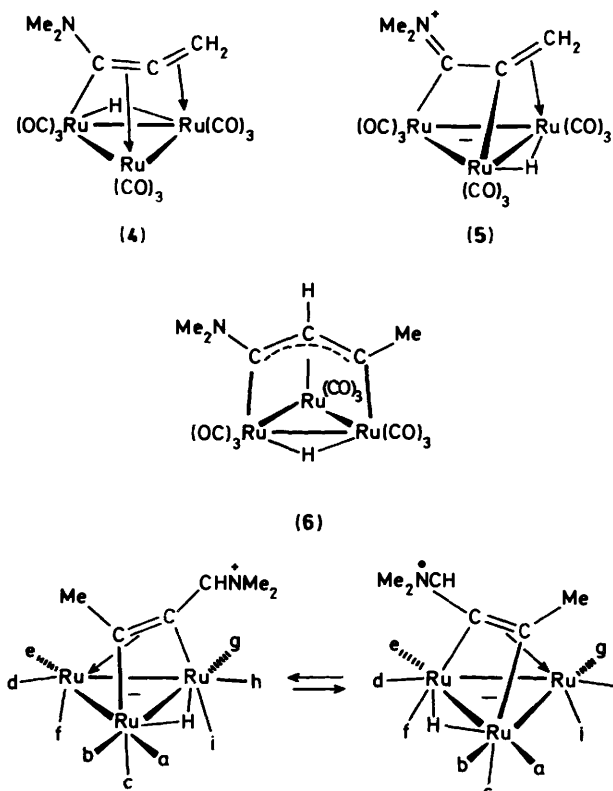
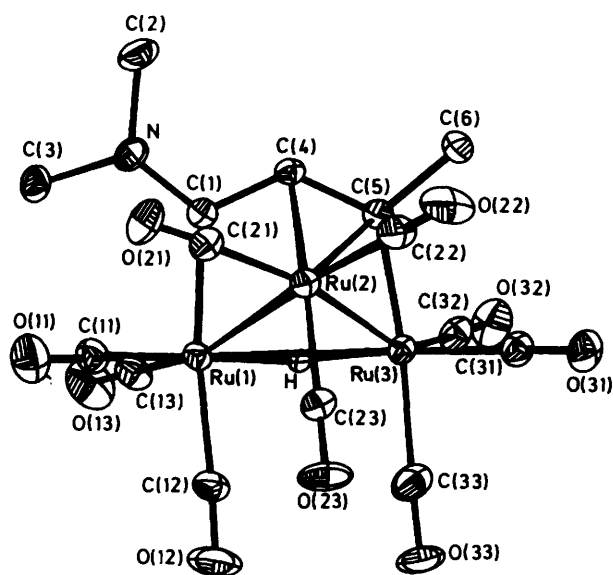
Ru(1)-Ru(2)	2.723(1)	Ru(3)-Ru(2)	2.742(1)
Ru(1)-Ru(3)	2.978(1)	C(1)-Ru(1)	2.130(5)
H-Ru(1)	1.688(17)	C(5)-Ru(3)	2.070(5)
H-Ru(3)	1.689(15)	C(2)-N(1)	1.298(5)
C(3)-N(1)	1.456(6)	C(4)-N(1)	1.481(6)
C(2)-C(1)	1.435(5)	C(5)-C(1)	1.385(5)
C(6)-C(5)	1.512(7)	C(1)-Ru(2)	2.185(5)
C(5)-Ru(2)	2.261(5)	H(2)-C(2)	0.935(16)
C(11)-Ru(1)	1.906(5)	C(21)-Ru(2)	1.909(6)
C(12)-Ru(1)	1.922(6)	C(22)-Ru(2)	1.885(6)
C(13)-Ru(1)	1.932(6)	C(23)-Ru(2)	1.894(6)
Average CO	1.139(11)	C(31)-Ru(3)	1.907(6)
		C(32)-Ru(3)	1.946(6)
		C(33)-Ru(3)	1.879(6)
Ru(3)-Ru(1)-Ru(2)	57.3(1)	Ru(1)-Ru(3)-Ru(2)	56.7(1)
Ru(1)-Ru(2)-Ru(3)	66.1(1)	C(11)-Ru(1)-Ru(2)	91.4(2)
C(12)-Ru(1)-C(1)	104.4(2)	C(11)-Ru(1)-C(1)	96.1(2)
C(13)-Ru(1)-Ru(2)	104.7(2)	C(12)-Ru(1)-Ru(3)	111.5(2)
C(13)-Ru(1)-C(12)	97.9(3)	C(12)-Ru(1)-C(11)	97.3(3)
C(1)-Ru(1)-Ru(3)	65.8(2)	C(13)-Ru(1)-Ru(3)	96.6(2)
H-Ru(1)-Ru(3)	28.1(4)	C(13)-Ru(1)-C(11)	91.0(3)
H-Ru(1)-C(11)	174.0(7)	C(1)-Ru(1)-Ru(2)	51.8(2)
H-Ru(1)-C(13)	85.2(8)	H-Ru(1)-C(12)	87.8(6)
C(22)-Ru(2)-Ru(3)	98.9(2)	C(21)-Ru(2)-Ru(1)	98.3(2)
C(23)-Ru(2)-Ru(1)	89.8(2)	C(22)-Ru(2)-C(21)	95.4(3)
C(23)-Ru(2)-C(21)	97.9(3)	C(23)-Ru(2)-Ru(3)	87.7(2)
C(31)-Ru(3)-Ru(1)	110.2(2)	C(33)-Ru(3)-C(5)	92.8(2)
C(31)-Ru(3)-C(5)	96.3(3)	C(33)-Ru(3)-C(32)	92.9(3)
C(32)-Ru(3)-Ru(2)	108.4(2)	C(5)-Ru(3)-Ru(2)	53.9(2)
C(32)-Ru(3)-C(31)	100.5(3)	C(32)-Ru(3)-Ru(1)	97.3(2)
C(33)-Ru(3)-Ru(2)	92.8(2)	H-Ru(3)-C(31)	88.4(7)
C(33)-Ru(3)-C(31)	96.0(3)	H-Ru(3)-C(33)	175.1(7)
C(5)-Ru(3)-Ru(1)	69.6(2)	H-Ru(3)-C(32)	84.1(9)
H-Ru(3)-Ru(1)	28.1(5)	C(4)-N(1)-C(2)	121.2(4)
C(3)-N(1)-C(2)	122.7(4)	C(2)-C(1)-Ru(2)	130.4(2)
C(4)-N(1)-C(3)	115.9(4)	C(5)-C(1)-C(2)	131.9(3)
C(5)-C(1)-Ru(2)	74.9(3)	C(1)-C(5)-Ru(3)	110.5(3)
C(1)-C(2)-N(1)	124.3(4)	C(6)-C(5)-C(1)	121.8(4)
C(6)-C(5)-Ru(3)	127.4(3)	C(22)-Ru(2)-C(1)	117.1(3)
Ru(1)-H-Ru(3)	123.8(10)	C(23)-Ru(2)-C(1)	139.0(2)
C(21)-Ru(2)-C(5)	124.6(3)	C(1)-Ru(2)-Ru(1)	50.0(2)
C(22)-Ru(2)-C(5)	90.0(3)	C(5)-Ru(2)-Ru(1)	72.7(2)
C(23)-Ru(2)-C(5)	135.4(2)	C(5)-Ru(2)-C(1)	36.3(1)
C(1)-Ru(2)-Ru(3)	70.1(2)	C(2)-C(1)-Ru(1)	111.4(3)
C(5)-Ru(2)-Ru(3)	47.7(1)	Ru(3)-C(5)-Ru(2)	78.4(2)
Ru(1)-C(1)-Ru(2)	78.2(2)	C(6)-C(5)-Ru(2)	124.3(3)
C(5)-C(1)-Ru(1)	114.0(3)		
C(1)-C(5)-Ru(2)	68.9(3)		

oscillation as illustrated. The enantiomer on the left-hand side of the Scheme 2 corresponds with that displayed for compound (1) and in Figure 1. Note that the small twist of the  $\mu_3$  ligand in the crystal is in the direction required for this oscillation. Finally at  $+90$  °C a  $^{13}\text{C}$  n.m.r. singlet is observed indicating the total exchange of CO ligands. Various mechanisms could account for this, including CO migration between metal atoms, but we

**Table 2.**  $^{13}\text{C}$  N.m.r. data for the CO ligands of compounds  $[\text{Ru}_3\text{H}(\text{MeC}=\text{CCH}=\text{NMe}_2)(\text{CO})_9]$  (1) and  $[\text{Ru}_3\text{H}(\text{MeC}=\text{CHC}=\text{NMe}_2)(\text{CO})_9]$  (2) enriched in  $^{13}\text{C}$  and recorded in  $\text{CD}_2\text{Cl}_2$  at  $-85^\circ\text{C}$  (1) and  $-58^\circ\text{C}$  (2)\*

Compound	a	b	c	d	e	f	g	h	i
(1)	193.8	194.7	199.6	195.5	193.8	207.8	195.9	190.7	201.1
(2)	193.6	189.6	199.5	194.7	191.4	207.7	191.4	193.6	197.7

\* The assignments for d and e might be reversed for either compound. The b and g assignments are supported by coupling to the hydride in the absence of proton decoupling.

**Scheme 2.****Figure 2.** Structure of  $[\text{Ru}_3\text{H}(\text{MeC}=\text{CHC}=\text{NMe}_2)(\text{CO})_9]$  (2)**Table 3.** Selected bond lengths ( $\text{\AA}$ ) and angles ( $^\circ$ ) for compound (2)

Ru(2)–Ru(1)	2.781(0.5)	Ru(3)–Ru(1)	2.968(0.5)
Ru(3)–Ru(2)	2.750(0.5)	C(5)–Ru(3)	2.061(6)
H–Ru(1)	1.587(22)	C(1)–Ru(1)	2.095(6)
H–Ru(3)	1.605(25)	C(4)–Ru(2)	2.296(5)
C(1)–N(1)	1.327(6)	C(1)–Ru(2)	2.689(6)
C(3)–N(1)	1.458(6)	C(5)–Ru(2)	2.248(5)
C(5)–C(4)	1.409(6)	C(11)–Ru(2)	1.889(5)
C(2)–N(1)	1.475(7)	C(12)–Ru(1)	1.938(7)
C(4)–C(1)	1.462(6)	C(13)–Ru(1)	1.916(6)
C(6)–C(5)	1.526(7)	C(21)–Ru(1)	1.896(6)
Average CO	1.137(10)	C(22)–Ru(2)	1.915(6)
		C(23)–Ru(2)	1.883(6)
		C(31)–Ru(3)	1.898(6)
		C(32)–Ru(3)	1.908(6)
		C(33)–Ru(3)	1.942(7)
Ru(3)–Ru(1)–Ru(2)	57.0(1)	Ru(3)–Ru(2)–Ru(1)	64.9(1)
Ru(2)–Ru(3)–Ru(1)	58.1(1)	C(11)–Ru(1)–Ru(2)	90.2(2)
C(11)–Ru(1)–Ru(3)	144.7(1)	C(11)–Ru(1)–C(1)	91.5(3)
C(12)–Ru(1)–Ru(2)	102.5(2)	C(12)–Ru(1)–Ru(3)	86.6(2)
C(12)–Ru(1)–C(1)	167.8(2)	C(12)–Ru(1)–C(11)	88.7(3)
C(13)–Ru(1)–Ru(2)	162.2(1)	C(13)–Ru(1)–Ru(3)	116.6(2)
C(13)–Ru(1)–C(1)	98.9(3)	C(13)–Ru(1)–C(11)	98.6(3)
C(13)–Ru(1)–C(12)	93.2(3)	C(1)–Ru(1)–Ru(2)	65.2(2)
C(1)–Ru(1)–Ru(3)	86.2(2)	H–Ru(1)–Ru(2)	78.0(7)
H–Ru(1)–Ru(3)	21.7(6)	H–Ru(1)–C(11)	165.9(6)
H–Ru(1)–C(12)	86.5(9)	H–Ru(1)–C(13)	94.9(7)
H–Ru(1)–C(1)	90.4(9)	C(21)–Ru(2)–Ru(1)	96.6(2)
C(21)–Ru(2)–Ru(3)	161.3(1)	C(22)–Ru(2)–Ru(1)	170.8(1)
C(22)–Ru(2)–Ru(3)	106.2(2)	C(22)–Ru(2)–C(21)	92.2(3)
C(23)–Ru(2)–Ru(1)	85.0(2)	C(23)–Ru(2)–Ru(3)	81.3(2)
C(23)–Ru(2)–C(21)	100.6(3)	C(23)–Ru(2)–C(22)	96.3(3)
C(31)–Ru(3)–Ru(1)	148.2(1)	C(31)–Ru(3)–Ru(2)	92.9(2)
C(31)–Ru(3)–C(5)	91.4(3)	C(32)–Ru(3)–Ru(1)	116.6(2)
C(32)–Ru(3)–Ru(2)	150.4(1)	C(32)–Ru(3)–C(5)	97.9(3)
C(32)–Ru(3)–C(31)	95.0(3)	C(33)–Ru(3)–Ru(1)	92.1(2)
C(33)–Ru(3)–Ru(2)	113.6(2)	C(33)–Ru(3)–C(5)	166.9(2)
C(33)–Ru(3)–C(31)	88.0(3)	C(33)–Ru(3)–C(32)	95.2(3)
C(5)–Ru(3)–Ru(1)	81.5(2)	C(5)–Ru(3)–Ru(2)	53.4(2)
H–Ru(5)–Ru(1)	21.4(4)	H–Ru(3)–Ru(2)	78.8(6)
H–Ru(3)–C(5)	89.7(9)	H–Ru(3)–C(31)	168.7(4)
H–Ru(3)–C(32)	96.0(5)	H–Ru(3)–C(33)	88.3(9)
C(2)–N(1)–C(1)	123.8(4)	C(3)–N(1)–C(1)	123.7(4)
C(3)–N(1)–C(2)	112.4(4)	N(1)–C(1)–Ru(1)	127.6(4)
C(4)–C(1)–Ru(1)	116.5(4)	C(4)–C(1)–N(1)	115.5(4)
C(5)–C(4)–C(1)	125.7(4)	C(4)–C(5)–Ru(3)	126.1(4)
C(6)–C(5)–Ru(3)	121.7(4)	C(6)–C(5)–C(4)	112.1(4)
Ru(3)–H–Ru(1)	136.9(9)		

believe that the best explanation is a second oscillation totally analogous to that in Scheme 2 but with the reverse orientation of the alkyne; that is an oscillation with the  $\text{CHNMe}_2$ -substituted end of the alkyne fixed as a pivot and the  $\text{Me}$ -substituted end oscillating. A combination of these two oscillations would allow the alkyne to move between all three possible orientations it might adopt at the  $\text{Ru}_3$  triangle. Alkyne rotations in trinuclear clusters are now fully established in many cases, for example see ref. 6. Remembering that axial–equatorial CO site exchange at Ru(2) is very rapid, alkyne rotation would lead to total CO exchange.

**Table 4.** Crystallographic data for compounds  $[\text{Ru}_3\text{H}(\text{MeC}=\text{CCH}=\text{NMe}_2)(\text{CO})_9]$  (1) and  $[\text{Ru}_3\text{H}(\text{MeC}=\text{CHC}=\text{NMe}_2)(\text{CO})_9]$  (2)

Complex	(1)	(2)
Formula	$\text{C}_{15}\text{H}_{11}\text{NO}_9\text{Ru}_3$	$\text{C}_{15}\text{H}_{11}\text{NO}_9\text{Ru}_3$
<i>M</i>	652.47	652.47
Crystal system	Monoclinic	Monoclinic
<i>a</i> /Å	11.456(2)	7.211(2)
<i>b</i> /Å	9.417(1)	16.788(2)
<i>c</i> /Å	18.759(3)	17.198(3)
$\beta$ /°	92.35(1)	101.80(2)
<i>U</i> /Å <sup>3</sup>	2 021.222	2 037.782
Space group	$P2_1/n$	$P2_1/c$
<i>Z</i>	4	4
<i>D</i> <sub>c</sub> /g cm <sup>-3</sup>	1.944	1.928
<i>F</i> (000)	1 248	1 248
$\mu$ /cm <sup>-1</sup>	20.45	20.29
Crystal size/mm	0.58 × 0.35 × 0.05	0.52 × 0.25 × 0.10
$\theta$ range/°	1.5–27	1.5–25
No. of unique data	4 391	3 588
No. of observed data	3 766	3 211
Significance test	$F > 3\sigma(F_o)$	$F > 3\sigma(F_o)$
No. of parameters	288	297
Weighting scheme:		
coefficient <i>g</i> in $w = 1/[\sigma^2(F_o) + gF_o^2]$	0.001	0.0006
Final $R = \Sigma\Delta F/\Sigma F_o$	0.0308	0.0277
$R' = [\Sigma w\Delta F^2/\Sigma wF_o^2]^{1/2}$	0.0434	0.0408

**Structure and Dynamic Behaviour of Compound (2).**—The *X*-ray molecular structure of compound (2) is given in Figure 2 with selected bond lengths and angles given in Table 3. The structure is superficially similar to that expected for the allyl description (6) but the  $\mu_3$  ligand is bound very unsymmetrically. The Ru(2)–C(1) length of 2.689(6) Å is much too long for a bond so that there is a  $\eta^2$  rather than  $\eta^3$  interaction at Ru(2). As in cluster (1) the planarity of the C=NMe<sub>2</sub> group (sum of angles at nitrogen is 359.9°) and the short C(1)–N bond length of 1.327(6) Å fit the zwitterionic description given for (2). The  $\sigma$  Ru–C bonds in both compounds (1) and (2), ranging from 2.061 to 2.130 Å, are shorter than the Ru–C bonds in the  $\eta^2$  contacts which are in the range 2.185–2.296 Å, which is quite normal. As in compound (1) the longest Ru–CO bond lengths in (2) are those *trans* to the  $\sigma$  Ru–C bonds associated with the  $\mu_3$  ligand. These are 1.938(7) and 1.942(7) Å.

The dynamic behaviour observed in the <sup>13</sup>C n.m.r. spectrum of (2) involves only localised axial–equatorial CO exchange and no evidence for  $\mu_3$  ligand mobility as in (1). Exchange at the metal atom with the  $\eta^2$  contact is the fastest. Thus signals for carbonyls d, e, and f (194.7, 191.4, and 207.7 p.p.m.) coalescence between –58 and +15 °C gives a signal at 197.8 p.p.m. Coalescence of the signals for h, i, and g is at a rather higher temperature while the signals for a, b, and c do not coalesce even at +110 °C. Essentially this means that the  $\mu$ - $\eta^2$ -vinyl group in (2) is static unlike most other bridging vinyl ligands which readily oscillate. Typical examples of oscillating  $\mu$ - $\eta^2$ -vinyl ligands are those in  $[\text{Os}_3\text{H}(\mu\text{-}\eta^2\text{-CH}=\text{CH}_2)(\text{CO})_{10}]^{10}$  and  $[\text{Os}_3\text{H}(\mu\text{-}\eta^2\text{-CPh}=\text{CHPh})(\text{CO})_{10}]^{11}$ .

In some ways the dynamic behaviour of compounds (1) and (2) is similar to that of the corresponding hydrocarbon complexes. The 'allyl' forms,  $[\text{Ru}_3\text{H}_2(\mu_3\text{-}\eta^3\text{-MeCCHCR})(\text{CO})_9]$  (R = Me or Et), show localised scrambling of axial and equatorial CO ligands but no motion of the  $\eta^3$  ligand.<sup>1</sup> However, there is evidence for an oscillation of the allenyl ligand in  $[\text{Ru}_3\text{H}(\mu_3\text{-MeC}=\text{C}=\text{CMe}_2)(\text{CO})_9]$  which involves the  $\sigma$  Ru–C bond remaining intact while the CMe<sub>2</sub> end of the ligand oscillates between the other two Ru atoms.<sup>12</sup> Since the modes of bonding are so different when the NMe<sub>2</sub> group is introduced,

**Table 5.** Fractional atomic co-ordinates ( $\times 10^4$ ) for compound (1)

Atom	<i>x</i>	<i>y</i>	<i>z</i>
Ru(1)	7 773(0.5)	–314(0.5)	1 349(0.5)
Ru(2)	8 658(0.5)	2 356(0.5)	1 240(0.5)
Ru(3)	6 320(0.5)	2 159(0.5)	866(0.5)
O(11)	10 141(3)	–1 501(4)	1 842(2)
O(12)	6 288(3)	–2 628(4)	1 977(2)
O(13)	8 012(4)	–1 644(5)	–124(2)
O(21)	11 111(3)	1 795(5)	1 882(2)
O(22)	8 887(4)	5 561(4)	1 265(3)
O(23)	9 123(4)	1 817(5)	–310(2)
O(31)	3 847(3)	1 811(5)	1 354(2)
O(32)	6 064(4)	1 334(5)	–721(2)
O(33)	6 116(3)	5 308(3)	541(2)
N(1)	7 495(3)	585(3)	3 310(2)
C(1)	7 738(3)	1 373(3)	2 105(2)
C(2)	8 160(3)	920(3)	2 795(2)
C(3)	6 225(4)	640(5)	3 235(3)
C(4)	7 993(4)	1(5)	3 993(2)
C(5)	7 046(3)	2 511(4)	1 883(2)
C(6)	6 793(4)	3 729(4)	2 379(2)
C(11)	9 262(3)	–1 042(4)	1 666(2)
C(12)	6 838(4)	–1 783(4)	1 746(2)
C(13)	7 928(4)	–1 142(5)	417(2)
C(21)	10 197(3)	1 992(5)	1 635(2)
C(22)	8 802(4)	4 350(4)	1 255(3)
C(23)	8 952(4)	2 007(5)	270(2)
C(31)	4 752(3)	1 922(4)	1 142(2)
C(32)	6 148(4)	1 642(4)	–138(2)
C(33)	6 194(3)	4 111(4)	668(2)

**Table 6.** Fractional atomic co-ordinates ( $\times 10^4$ ) for compound (2)

Atom	<i>x</i>	<i>y</i>	<i>z</i>
Ru(1)	12 124(0.5)	3 145(0.5)	1 949(0.5)
Ru(2)	9 847(0.5)	4 028(0.5)	2 753(0.5)
Ru(3)	12 880(0.5)	3 284(0.5)	3 706(0.5)
O(11)	9 110(6)	3 234(3)	441(2)
O(12)	10 826(7)	1 426(2)	2 140(3)
O(13)	15 344(5)	2 610(3)	1 173(3)
O(21)	7 152(5)	4 658(2)	1 280(2)
O(22)	7 807(6)	4 958(2)	3 838(3)
O(23)	7 884(4)	2 464(2)	2 944(2)
O(31)	11 345(5)	3 527(2)	5 205(2)
O(32)	16 990(5)	3 304(3)	4 585(2)
O(33)	12 279(7)	1 492(2)	3 931(3)
N(1)	12 749(5)	4 830(2)	1 327(2)
C(1)	12 554(5)	4 379(2)	1 939(2)
C(2)	12 876(8)	5 707(3)	1 358(3)
C(3)	12 745(6)	4 518(3)	536(2)
C(4)	12 406(5)	4 811(2)	2 663(2)
C(5)	12 651(5)	4 479(2)	3 429(2)
C(6)	12 870(6)	5 118(2)	4 073(2)
C(11)	10 237(6)	3 202(3)	1 010(2)
C(12)	11 331(7)	2 062(3)	2 094(3)
C(13)	14 202(6)	2 813(3)	1 488(3)
C(21)	8 175(6)	4 424(3)	1 839(3)
C(22)	8 612(6)	4 623(2)	3 451(3)
C(23)	8 690(6)	3 044(3)	2 882(3)
C(31)	11 912(6)	3 451(3)	4 639(2)
C(32)	15 473(6)	3 282(3)	4 241(3)
C(33)	12 502(7)	2 150(3)	3 833(3)

the superficial similarity of behaviour should not be over emphasised.

Interestingly the zwitterionic character of compounds (1) and (2) is further corroborated by their electrochemical behaviour in non-aqueous solvents when compared with that of other compounds in the series  $[\text{Ru}_3\text{H}(\text{MeC}=\text{C}=\text{CHR})(\text{CO})_9]$  and  $[\text{Ru}_3\text{H}(\text{MeCCHCR})(\text{CO})_9]$  where R is a hydrocarbon group.

The presence of the dimethylamino group in (1) and (2) lowers the range of oxidation potentials and increases the range of reduction potentials, indicating a higher electron density localised in the metallic framework.<sup>13</sup>

### Experimental

Compounds (1) and (2) were synthesised as reported earlier<sup>5</sup> and crystals were obtained for X-ray structure determination from the evaporation of hexane solutions. Variable-temperature <sup>13</sup>C n.m.r. spectra of <sup>13</sup>C-enriched samples of compounds (1) and (2) were recorded in CD<sub>2</sub>Cl<sub>2</sub> from -85 to 21 °C and in [<sup>2</sup>H<sub>8</sub>]toluene up to 110 °C.

**Crystallographic Studies.**—Unit-cell and intensity data were obtained using an Enraf-Nonius CAD4 diffractometer (graphite monochromatized Mo-K<sub>α</sub> radiation, λ = 0.710 69 Å) in the ω-2θ scan mode. Methods used for data collection have been outlined in a previous publication.<sup>14</sup> Empirical absorption corrections were applied to the intensity data; an additional correction for absorption (DIFABS<sup>15</sup>) was made at the stage of isotropic refinement. Crystallographic data are listed in Table 4.

For both compounds the positions of the ruthenium atoms were obtained using direct methods.<sup>16</sup> Calculation of the difference-Fourier maps enabled location of the remaining atoms. Hydrogen atoms were located experimentally including the metal-bridging hydride ligands in each case. The final refinement by full-matrix least squares employed anisotropic thermal parameters, except those on C(3) of compound (1), which were refined as part of a rigid group, and assigned a group isotropic thermal parameter.

Final fractional co-ordinates for the two compounds are given in Tables 5 and 6. Figures 1 and 2 were drawn using SNOOPI.<sup>17</sup>

### Acknowledgements

We thank the S.E.R.C. for financial support.

### References

- 1 S. Aime, L. Milone, D. Osella, M. Valle, and E. W. Randall, *Inorg. Chim. Acta*, 1976, **20**, 217 and refs. therein.
- 2 M. I. Bruce, in 'Comprehensive Organometallic Chemistry,' eds. G. Wilkinson, F. G. A. Stone, and E. W. Abel, Pergamon Press, Oxford, 1982, ch. 32.5, p. 843; R. D. Adams and J. P. Selegue, *ibid.*, ch. 33.3, p. 1023.
- 3 G. Gervasio, D. Osella, and M. Valle, *Inorg. Chem.*, 1976, **15**, 1221.
- 4 M. Evans, M. B. Hursthouse, E. W. Randall, E. Rosenberg, L. Milone, and M. Valle, *J. Chem. Soc., Chem. Commun.*, 1972, 545.
- 5 S. Aime, G. Jannon, D. Osella, A. J. Arce, and A. J. Deeming, *J. Chem. Soc., Dalton Trans.*, 1984, 1987.
- 6 K. Henrick, M. McPartlin, A. J. Deeming, S. Hasso, and P. J. Manning, *J. Chem. Soc., Dalton Trans.*, 1982, 899.
- 7 J. R. Shapley, M. Tachikawa, M. R. Churchill, and R. A. Lashewycz, *J. Organomet. Chem.*, 1978, **162**, C39.
- 8 M. R. Churchill and R. A. Lashewycz, *Inorg. Chem.*, 1979, **18**, 848.
- 9 S. Aime, D. Osella, A. J. Arce, A. J. Deeming, M. B. Hursthouse, and A. M. R. Galas, *J. Chem. Soc., Dalton Trans.*, 1984, 1981.
- 10 J. R. Shapley, S. I. Richter, M. Tachikawa, and J. B. Keister, *J. Organomet. Chem.*, 1975, **94**, C43.
- 11 A. D. Clauss, M. Tachikawa, J. R. Shapley, and C. G. Pierpont, *Inorg. Chem.*, 1981, **20**, 1528.
- 12 S. Aime, R. Gobetto, D. Osella, L. Milone, and E. Rosenberg, *Organometallics*, 1982, **1**, 640.
- 13 P. Zanello, S. Aime, and D. Osella, *Organometallics*, 1984, **3**, 1374.
- 14 M. B. Hursthouse, R. A. Jones, K. M. A. Malik, and G. Wilkinson, *J. Am. Chem. Soc.*, 1979, **101**, 4128.
- 15 N. Walker and D. Stuart, *Acta Crystallogr., Sect. A*, 1983, **39**, 158.
- 16 G. M. Sheldrick, SHELX 76 program for crystal structure determination, University of Cambridge, 1976.
- 17 E. K. Davis, SNOOPI program for drawing molecular structures, University of Oxford, 1983.

Received 1st October 1985; Paper 5/1702